sustainability

MDPI

Article

Analysis and Simulation of Land Use Changes and Their Impact on Carbon Stocks in the Haihe River Basin by Combining LSTM with the InVEST Model

Yanzhen Lin, Lei Chen *, Ying Ma and Tingting Yang

College of Geography and Environmental Science, Tianjin Normal University, Tianjin 300387, China; lyz0212022@163.com (Y.L.); maying100105@163.com (Y.M.); ytt0206mut@163.com (T.Y.)
* Correspondence: lchen@tjnu.edu.cn; Tel.: +86-130-1225-0737

Abstract: The quantitative analysis and prediction of spatiotemporal patterns of land use in Haihe River Basin are of great significance for land use and ecological planning management. To reveal the changes in land use and carbon stock, the spatial–temporal pattern of land use data in the Haihe River Basin from 2000 to 2020 was studied via Mann–Kendall (MK) trend analysis, the transfer matrix, and land use dynamic attitude. Through integrating the models of the Integrated Valuation of Ecosystem Services and Trade-offs (InVEST) and the Long Short-Term Memory (LSTM), the results of the spatial distribution of land use and carbon stock were obtained and compared with Cellular Automation (CA-Markov), and then applied to predict the spatial distribution in 2025. The results show the following: (1) The land use and land cover (LULC) changes in the Haihe River Basin primarily involve an exchange between cultivated land, forest, and grassland, as well as the conversion of cultivated land to built-up land. This transformation contributes to the overall decrease in carbon storage in the basin, which declined by approximately 1.20% from 2000 to 2020. (2) The LULC prediction accuracy of LSTM is nearly 2.00% higher than that of CA-Markov, reaching 95.01%. (3) In 2025, the area of grassland in Haihe River Basin will increase the most, while the area of cultivated land will decrease the most. The spatial distribution of carbon stocks is higher in the northwest and lower in the southeast, and the changing areas are scattered throughout the study area. However, due to the substantial growth of grassland and forest, the carbon stocks in the Haihe River Basin in 2025 will increase by about 10 times compared with 2020. The research results can provide a theoretical basis and reference for watershed land use planning, ecological restoration, and management.

Keywords: land use; spatial and temporal characteristics; trend prediction; Haihe River Basin

Citation: Lin, Y.; Chen, L.; Ma, Y.; Yang, T. Analysis and Simulation of Land Use Changes and Their Impact on Carbon Stocks in the Haihe River Basin by Combining LSTM with the InVEST Model. *Sustainability* **2024**, *16*, 2310. https://doi.org/10.3390/su16062310

Academic Editors: Fabio Carlucci and Tommaso Caloiero

Received: 8 January 2024
Revised: 2 March 2024
Accepted: 8 March 2024
Published: 11 March 2024

1. Introduction

As an important component of ecosystem services, carbon storage is considered to be the most practical and environmentally friendly way to reduce the greenhouse effect, and is essential for assessing the health of regional ecosystems, developing appropriate conservation measures, and promoting regional sustainable development [1,2]. Some researchers have proposed that land use and land cover (LULC) is closely related to the changes in terrestrial ecological carbon storage and distribution. Different ground materials have various carbon sequestration capacities, which is an important factor in the carbon storage and transfer of the entire ecosystem [3]. Therefore, accurately analyzing and predicting the regional land use and distribution will help to understand the changes in the spatial and temporal distribution pattern of local carbon stocks, helping to realize the goals of carbon peak and carbon neutrality in the region [4].

The dynamic characterization of land use quantitatively describes the change rate of land use, playing a crucial role in predicting the future trajectory of land use change [5]. Landscape pattern indices, combining spatial analysis with ecology, offer a novel perspective for analyzing regional land use changes [6]. These factors are commonly employed

to analyze the spatial and temporal evolution characteristics, as well as the amplitude of changes in regional land use. Wang You et al. [7] selected three remote sensing images of Jingtai County from 2000, 2010, and 2020 to analyze the change rates in six land use types. Liu Yi [8] utilized land use change amplitude and the land use transfer matrix to quantitatively analyze the evolution patterns in the Lvshuijiang Basin. Additionally, Lian Hugang et al. [9] used the landscape pattern index to examine the spatiotemporal variations and correlations with windbreak and sand-fixation services over 20 years in the local area.

Many eco-system process models and empirical models have been developed for estimating carbon stocks, such as the BIOME-BGC Model [10] and the Terrestrial Ecosystem Model (TEM) [11]. These models require a large number of input parameters and obtain local meteorological data based on specific vegetation ecological data, which limits their universality. The Integrated Valuation of Ecosystem Services and Trade-offs (InVEST) model can stimulate ecosystem changes under different land cover scenarios and has been widely used to map the carbon storage of local terrestrial ecosystems [12]. Piyathilake [13] utilized the InVEST model to model and estimate carbon storage in Uva Province, Sri Lanka. Li et al. [14] applied the InVEST model's water quantity module to analyze the spatiotemporal dynamics of water conservation from 2000 to 2019 and its response to climate, land use, and soil changes. However, due to the dependency on LULC data, carbon stock estimations made by the InVEST model are greatly affected by the accuracy of LULC data.

Currently, major models used for land use change prediction include the Markov Chain model (MC) [15], Conversion of Land Use and its Effects model (CLUE) [16], Cellular Automata model (CA) [17], and Patch-generating Land Use Simulation (PLUS) model [18]. Among them, the CLUE model is inefficient [19], and the PLUS model primarily focuses on simulating patch-level changes [20]. The MC can quantitatively predict the future area of each land use type, but it cannot forecast the spatial distribution, while the CA model can achieve the opposite. It can predict spatial distribution but does not consider socio-economic factors [21]. Therefore, researchers combine CA with Markov coupling with socio-economic factors to model the spatiotemporal dynamics in land use. Based on the land use data of Jilin Province from 2011 to 2020, Wei Mengqi et al. [22] used the CA-Markov model to predict land use types and carbon sink changes in 2030 based on land use data from Jilin Province for 2011–2020. With an increase in data types, deep learning methods, specifically Long Short-Term Memory (LSTM), have been widely used in land use change prediction for long time series. Wang Jiaojiao et al. [23] selected Manas's land use remote sensing spatiotemporal data from 1992 to 2020 to compare the land use prediction accuracy of the LSTM model with that of CA-Markov and MLP-ANN models. The study demonstrated that LSTM has higher reliability and further used the LSTM model to predict the spatial distribution of land use in Manas in 2025. Also, LSTM can integrate with other models, like Convolutional Neural Networks (CNN) and CA, to improve the predicting accuracy. Xing Weiran et al. [24] introduced a novel model that integrates these networks, and used the CNN-LSTM-CA model to simulate the land use distribution of Dongguan City in 2014. Zhou Ye et al. [25] applied this to the area of Hangzhou City in 2020. Both of them achieved a simulation accuracy of 95.00%. These results validate the effectiveness and superiority of LSTM in accurately predicting land use patterns. Therefore, taking advantage of LSTM and InVEST models can realize the dual optimization of the structure and organization of regional land, and maximize the accuracy of future carbon storage predictions in the region. However, the application of LSTM is mainly concentrated in small- and medium-scale simulations, and its applicability at the basin scale is less verified.

Due to the acceleration of economic development and urbanization, the ecological environment of the Haihe River basin is in a fragile situation, facing wetland shrinkage, habitat barriers, and other ecological environmental problems [26]. Accurately simulating the land use changes in the Haihe River Basin will contribute to sustainable land use development and provide a theoretical reference for ecological adjustment and optimization. Taking advantage of the LSTM and InVEST model, we aim to (1) explore the spatiotemporal

evolution characteristics and trends of land use in Haihe River Basin from 2000 to 2020 in depth via the land use dynamic attitude and landscape pattern index; (2) calculate the carbon density of land use types in the Haihe Basin River, using the InVEST model to analyze the impact of land use changes on the ecosystem carbon storage; (3) compare the LSTM model with the CA-Markov model in the simulation of land use distribution of the Haihe River Basin in 2020, and predict the carbon storage in 2025 to offer a theoretical reference for ecological management.

2. Materials and Methods

2.1. Study Area and Data Sources

Haihe River Basin is one of the seven major river basins in China, situated in the eastern part of the country, covering a total area of 442,000 km^2. As of 2020, the predominant land use types in Haihe River Basin are cultivated land, forest, and grassland, constituting 45.60%, 21.30%, and 16.70% of the total area, respectively. Cultivated land is predominantly found in the eastern region of the basin, while forest and grassland are primarily distributed in the northwest and southeast regions. The range of study areas is shown in Figure 1. In this study, the land use type maps of Haihe River Basin spanning the period from 2000 to 2020 were selected. The land types include forest, water, built-up land, shrub, grassland, barren, wetland, cultivated land, and others.

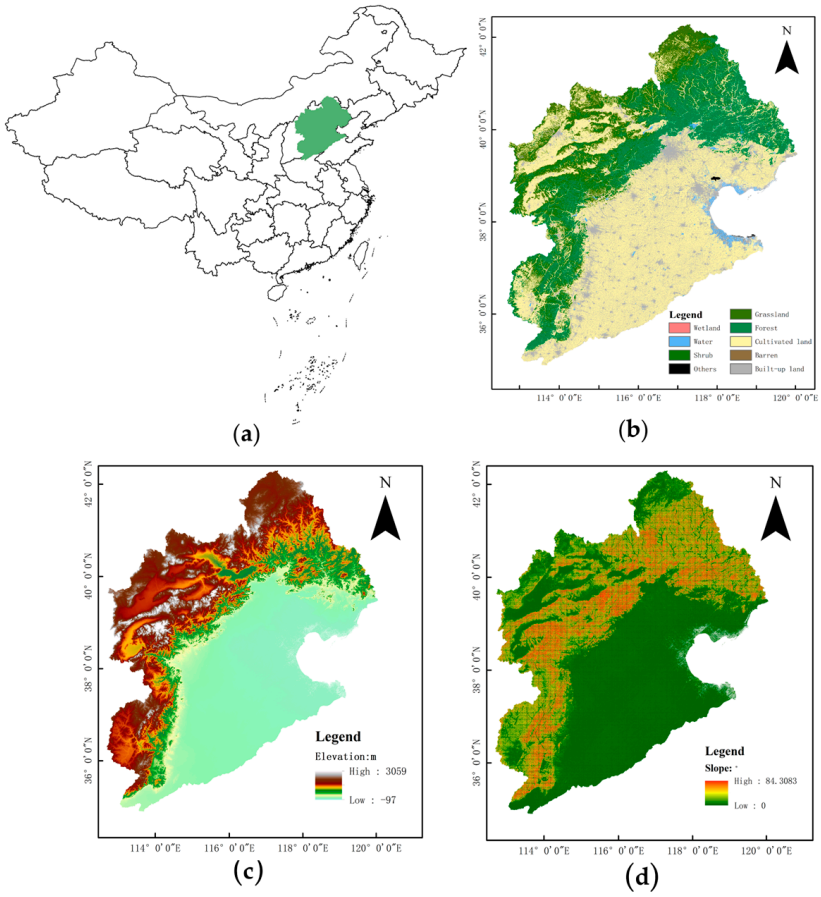

Figure 1. (**a**) Location map of study area; (**b**) slope of study area; (**c**) land use map in 2020 of study area; (**d**) DEM of study area.

We also considered other geographical data (Table 1). The geographical data incorporated three distance variables, namely the distance from motorways, railways, and primary roads. Additionally, natural element data were included, encompassing the Digital Elevation Model (DEM), slope, as well as relevant temperature and precipitation data.

Table 1. Details of data sources.

Data Type	Sources
LULC in Haihe River Basin from 2000 to 2020	CLCD from 1985 to 2021 (https://doi.org/10.5281/zenodo.5816591, accessed on 13 July 2023)
DEM and Slope	Resource and Environmental Science and Data Center of the Chinese Academy of Sciences (https://www.resdc.cn/, accessed on 1 August 2023)
Motorway, railway, and primary network	Geographic Information Professional Knowledge Service System
Precipitation and temperature	CRU TS (https://crudata.uea.ac.uk/cru/data/hrg/, accessed on 10 August 2023)
Carbon density in Chinese terrestrial ecosystems [27]	http://www.cnern.org.cn/data/meta?id=40579 http://www.sciencedb.cn/dataSet/handle/603, (accessed on 13 August 2023)

2.2. Methods

2.2.1. Analysis of LULC Dynamics

This paper employs the MK trend analysis, coupled with land use dynamic attitude and the land transfer matrix, to scrutinize the characteristics of land use changes.

(1) MK Trend Analysis

MK trend analysis is a statistical method commonly used to detect trends in time series data. The S-statistic and the normal distribution correction factor Z are used to determine whether the data show an increasing or decreasing trend and the significance of the trend. Generally speaking, if the absolute value of Z is greater than 1.96, that is, $Z > 1.96$ or $Z < -1.96$, then the trend can be considered significant. The formula for calculating S and Z is as follows:

$$S = \sum_{i=1}^{n-1} \sum_{j=i+1}^{n} sign(x_j - x_i), \quad (1)$$

where $sign(x_j - x_i)$ is a symbolic function, representing the positive and negative of $x_j - x_i$, the positive S statistic represents the increasing trend, and the negative S statistic represents the decreasing trend.

When $S > 0$,

$$Z = \frac{S-1}{\sqrt{V(S)}}, \quad (2)$$

When $S < 0$,

$$Z = \frac{S+1}{\sqrt{V(S)}}, \quad (3)$$

where S is the value of the S statistic and $V(S)$ is the variance of the S statistic.

(2) LULC dynamics attitude

Land use dynamic attitude represents the quantitative change in land use types that occurs within a certain time range, including single dynamic attitude and comprehensive dynamic attitude. Single dynamic attitude reflects the rate of change of a certain land use type in a certain period, and comprehensive dynamic attitude reflects the rate of change of all land use types. The formula of single dynamic attitude and comprehensive dynamic attitude is as follows:

$$K = \frac{U_i - U_j}{U_i} \times \frac{1}{T} \times 100\%, \quad (4)$$

where K is the dynamic attitude of a certain land use type, that is, the annual change rate; U_i represents the area of a certain land use type; and U_j represents the unchanged area of

a certain land use type. T is the length of the study period. The comprehensive dynamic attitude of the study area is calculated by Formula (5).

$$L = \frac{\sum_{i=1}^{n} |U_i - U_j|}{\sum_{i=1}^{n} U_i} \times \frac{1}{T} \times 100\%, \quad (5)$$

where U_i represents the area of a certain type of land use, U_j represents the unchanged area of a certain type of land use, n is the number of land use types, and T is the length of the study period.

(3) Transfer matrix

The land use transfer matrix is a form of static data that can reflect the coverage area of different land use types within a fixed period, and the dynamic changes between them can be projected in the form of a two-dimensional matrix. The formula is as follows:

$$S_{ij} = \begin{bmatrix} S_{11} & \cdots & S_{1n} \\ \vdots & \ddots & \vdots \\ S_{n1} & \cdots & S_{nn} \end{bmatrix}, \quad (6)$$

where S represents area; n is the number of land use types; S_{ij} is the conversion area of Class i land and Class j land (i, j = 1, 2... n); i and j are the types of land use before and after the transfer.

2.2.2. Analysis of Landscape Pattern Dynamics

The landscape pattern index provides a quantitative analysis of the organization and spatial structure of land cover types, which helps to understand the complexity and variation of land surface characteristics. Here, we selected six representative landscape indices (Table 2).

Table 2. Landscape indices and their significance.

Index Type	Index Significance
Total Edge (TE)/m	Used to measure marginal diversity within ecosystems, LSI can be combined to further assess landscape complexity.
Largest Patch Index (LPI)/%	Used to assess the impact of human activities on landscape changes and ecosystem integrity.
Landscape Shape Index (LSI)/%	Used to describe the shape complexity of patches in ecological landscapes and reveal the degree of fragmentation of habitats
Interspersion and Juxtaposition Index (IJI)/%	Used to evaluate the degree of interlace and juxtaposition of different habitat types in the landscape, to reflect the spatial pattern and complexity of the habitat.
Proportion of Like Adjacency (PLADJ)/%	Used to comprehensively consider the spatial distribution, proximity, and similarity among habitat types.
Numbers of Patch (NP)/n	Used to measure the degree of dispersion and fragmentation of different habitat types in an ecological landscape.

2.2.3. Carbon Storage Estimation with the InVEST Model

The carbon module in the InVEST model is used to calculate carbon storage by combining the land use and carbon density data of the Haihe River basin. The formula is as follows:

$$C_i = C_{above} + C_{blow} + C_{soil} + C_{dead}, \quad (7)$$

$$C_{total} = \sum_{i=1}^{n} A_i C_i$$

where C_i represents the carbon density of land use i; C_{above}, C_{blow}, C_{soil}, and C_{dead} represents the soil organic carbon pool; C_{total} represents ecosystem carbon storage; A_i represents the area of land use i; n represents the number of land use types.

Due to the different carbon densities of different land use types in different regions, this paper prioritizes the regional carbon density data in Haihe River Basin and then supplements them with national data to obtain preliminary carbon density data for the study area [28–30]. Carbon density data can be modified using temperature and precipitation data, and the correction formulas are as follows [31,32]:

$$C_{SP} = 3.3968 \times MAP + 3996.1, \tag{8}$$

$$C_{BP} = 6.798 \times e^{0.0054 \times MAP}, \tag{9}$$

$$C_{BT} = 28 \times MAT + 398, \tag{10}$$

$$K_B = K_{BP} \times K_{BT} = \frac{C_{BPhh}}{C_{BPchina}} \times \frac{C_{BThh}}{C_{BTchina}}, \tag{11}$$

$$K_S = \frac{C_{SPhh}}{C_{SPchina}}, \tag{12}$$

where MAT and MAP represent average annual temperature and interannual precipitation. C_{SP} is the soil carbon density obtained from precipitation data. C_{BP} and C_{BT} represent vegetation carbon density obtained from precipitation data and temperature data. K_B stands for vegetation correction coefficient; K_S represents the soil correction coefficient, and the carbon density table of different land use types in Haihe River Basin is obtained based on the above. The initial carbon density data can be multiplied by the correction coefficient to obtain the final carbon density data of the study area (Table 3).

Table 3. The carbon density for land use type in Haihe Basin River (Mg/ha).

Land Use Type	C_Above	C_Below	C_Soil	C_Dead
Others	0	0	0	0
Forest	18.72	51.18	215.25	13.49
Water	0	0	0	0
Built-up land	0	0	70.87	0
Shrub	23.33	15.21	288.98	21.09
Grassland	15.59	38.2	90.77	10.09
Barren	0	0	0	0
Wetland	0.55	1.81	23.69	0.12
Cultivated land	2.52	35.64	98.50	9.39

2.2.4. LSTM Spatial Prediction Model

LSTM is an improvement that can solve the problem of gradient explosion and gradient disappearance in RNN. Through gate units (forgetting gate, updating gate, and output gate), not only is the input information selectively retained, to achieve the purpose of forgetting unimportant noise and other information, but the new memory that is generated can be retained and deleted independently. Through LSTM, each pixel can be converted into the probability of changing into each type of land use. [23]. Wang X et al. [24] proposed that further screening of the LSTM results using the Random Forest (RF) model could achieve higher accuracy. Therefore, in this paper, CA and RF are used to further screen the probability obtained by LSTM.

Here, the LSTM model was trained using time series land use (LU) data and driving factors from 2000 to 2014 as the input data, while land-use-type data from 2005 to 2014 served as the output data to obtain the initial transfer probability data. Subsequently, Random Forest (RF) and Cellular Automata (CA) were employed to further screen the initial transfer probability data. During the training of the RF model, land use data and driving factors from 2009 were utilized as the input data, with the pixels that changed

from 2009 to 2014 serving as output data to predict future changes. Following this, CA was applied to assess the pixels individually. The pixels were identified to change not only under RF prediction but also under LSTM prediction, and those with an initial transfer probability greater than 0.80 were deemed to be transformed into the corresponding land use data. The model architecture includes two LSTM layers and one fully connected layer. Dropout was set to 0.20 in the fully connected layer to prevent overfitting. The chosen activation function was softmax, while Root Mean Square Propagation served as the optimizer, and Cross-Entropy (CE) was used as the loss function. The code implementation was carried out using the TensorFlow and Keras modules in Python. By inputting the land use map predicted by LSTM+RF+CA and the corrected carbon density values for each land use type from Table 3 into the InVEST model, the carbon storage map of the Haihe River Basin for the years 2020 and 2025 can be obtained.

3. Results

3.1. Dynamic Characteristics of LULC

An MK trend analysis was conducted on the land use data from 2000 to 2020 to quantitatively characterize the changes. Figure 2 illustrates that forest, water, built-up land, and wetland areas generally increased, whereas shrub, grassland, barren, and cultivated land areas decreased. Particularly noteworthy are the significant changes observed in built-up land, forest, and cultivated land. The increasing trend in built-up land area is particularly notable, while the cultivated land area shows the most pronounced decline.

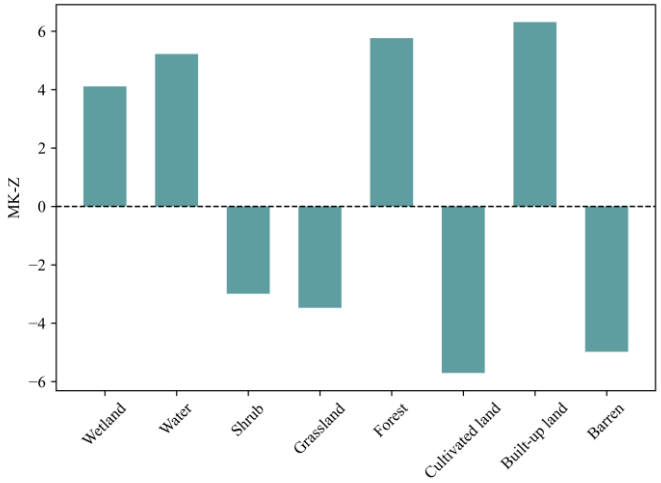

Figure 2. MK trend analysis.

Based on the area of each type of land use, calculations of the individual dynamics of each type of land use, and the comprehensive dynamics of the Haihe River Basin, the speed of their change can be obtained, as shown in Figures 3 and 4. Due to the significant variations in the dynamic attitude value of different land use types, Figure 3 is divided into two parts to clearly depict the changing trends of each type. An examination of the annual area change rates for forest, cultivated land, and built-up land, which experienced the most significant alterations, reveals notable trends. Between 2000 and 2001, there was a sharp decline in the growth rate of built-up land. Subsequently, from 2002 to 2020, a consistently low growth rate persisted. The rate of cultivated land reduction declined from 2000 to 2001 and stabilized by 2016. In the years 2017–2018, cultivated land transitioned from a decrease to an increase, with an accelerated growth rate. However, in 2019–2020, the pace of cultivated land recovery decelerated. The forest area exhibited a downward trend from 2000 to 2001, followed by an upward trajectory from 2001 to 2020, maintaining a relatively stable growth rate until 2020.

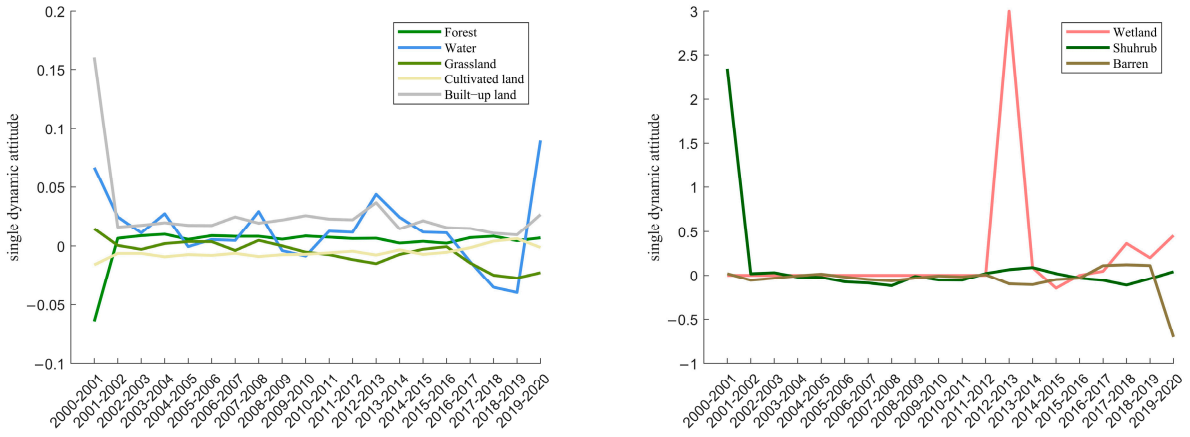

Figure 3. Single dynamic attitude of LULC.

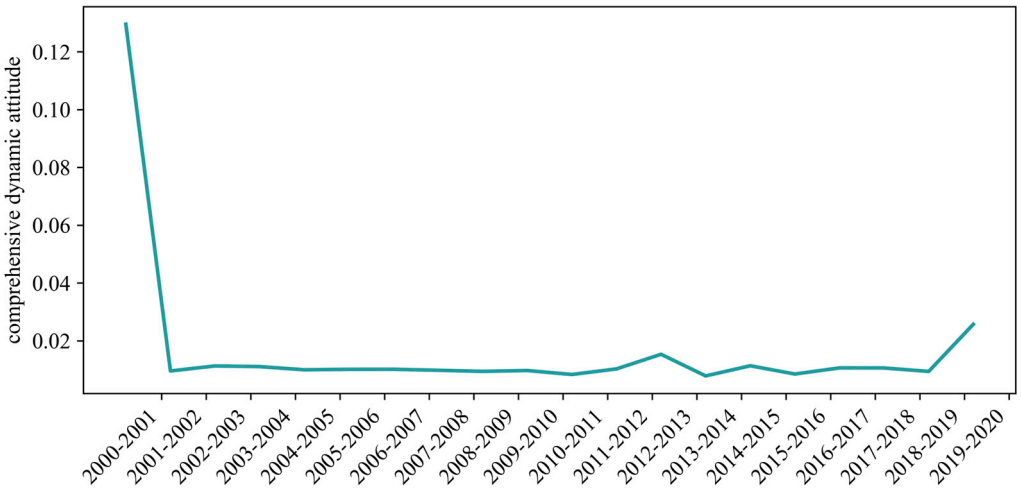

Figure 4. Comprehensive dynamic attitude of LULC.

The analysis of the change in comprehensive dynamic attitude (Figure 4) illustrates that the most significant alteration occurred from 2000 to 2001, followed by a slight increase from 2018 to 2020. Figure 3, and the relevant data, make evident that the decrease that occurred from 2000 to 2001 correlates closely with the sharp decline in the growth rate of built-up land and shrub area, while the increase from 2018 to 2020 is linked to the drastic changes in water and wetland in 2018.

The annual land transfer matrix is visualized as a Sankey diagram (Figure 5) which depicts the specific changes in each land use category from 2000 to 2020. Notably, the most substantial change occurred between 2000 and 2001, where 16.70% of forest transitioned to other land use categories, while 11.30% converted to grassland. Additionally, during this period, there was a transition from some grassland to forest and cultivated land, alongside the conversion of cultivated land to built-up land. Furthermore, the shift from seven to eight main land use types between 2012 and 2013, attributed to the emergence of wetlands, is noteworthy. A detailed analysis reveals that a minor portion of water was converted to wetland in 2011.

The expansion in cultivated land area in 2017–2018, analyzed in conjunction with Figures 3 and 5, was attributed to the conversion of 2.00% of grassland into cultivated land, while the subsequent decrease in 2019 was caused by the conversion of 1.00% of cultivated land into built-up land and grassland. The growth in forest area resulted from a 0.70% conversion of grassland to forest. Upon examining Figures 4 and 5, the significant fluctuations in 2000–2001 were driven by shrub migration, with 19.60% of shrubland converting to forest. The alterations observed during 2019–2020 were influenced by the

combined effects of wetland and barren land. According to Figure 5, a considerable portion of barren was transformed into water and built-up areas, with 40.30% of the total barren being converted into water and 30.00% into built-up areas.

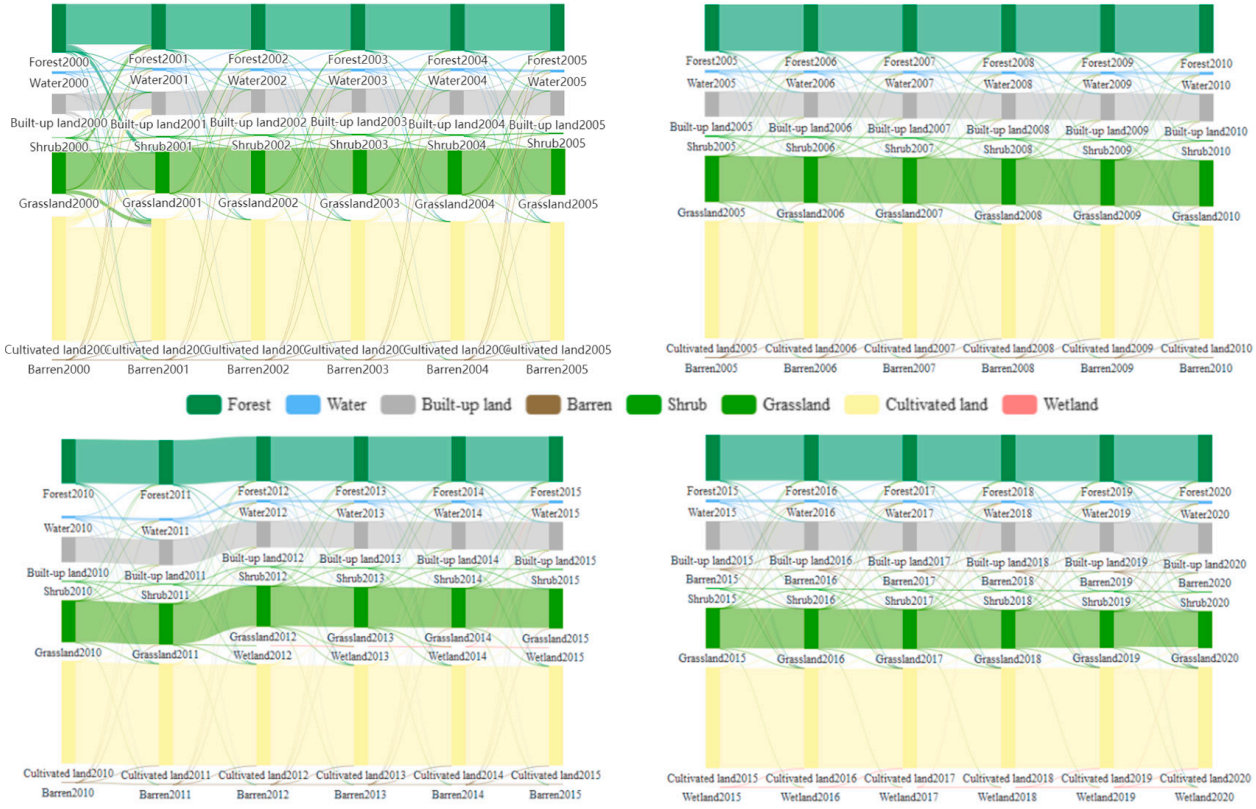

Figure 5. Transfer matrix of LULC changes in Haihe River Basin from 2000 to 2020.

3.2. Pattern Dynamics of Characteristics of LULC

The annual land use map was processed using Fragstats4.2 (https://fragstats.org/index.php/downloads, accessed on 1 January 2024), which is a powerful software used for calculating landscape indices, to derive the landscape indices for each LULC, and subsequent statistical analysis yielded Figure 6, which shows that NP, TE, LSI, PLADJ, and IJI can be roughly divided into two stages. In the early stage, from 2000 to 2001, there was a significant change in landscape indices, while in the later stage, from 2001 to 2020, the landscape indices changed steadily. The NP, TE, and LSI values for each land use type showed dramatic increases from 2000 to 2001, indicating increased fragmentation for each land use type. Among them, the NP of forest, shrub, and grassland increased significantly by 326.52%, 726.95%, and 352.76%, respectively. Combining the changes in LSI and TE can illustrate the complexity of land use shapes. According to Figure 6, during 2000–2001, the complexity of land use shapes in the Haihe River Basin deepened for each land use type, particularly in forest and grasslands. Forest LSI increased by 145.13%, TE increased by 137.60%, grassland LSI increased by 136.68%, and TE increased by 138.70. The PLADJ for each land use type showed a declining trend, indicating a decrease in aggregation for each land type, with the aggregation of barren land witnessing the most drastic decline, dropping by 14.61%. Except for water and barren land, the IJI of other land uses showed an increasing trend, indicating that, from 2000 to 2001, the shapes of other land uses tended to be similar in the Haihe River Basin, which showed a decreasing trend. These changes are related to the urbanization process in the Haihe River Basin, indicating the environmental damage and interference caused by human construction activities from 2000 to 2001.

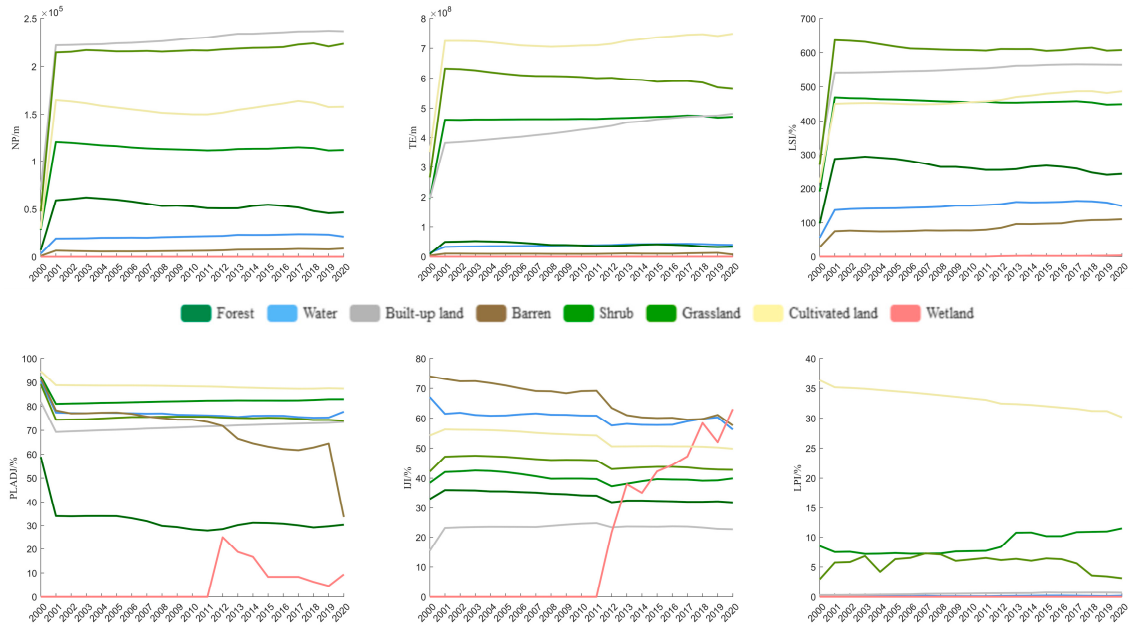

Figure 6. Landscape indices of LULC.

From 2001 to 2020, the NP, TE, and LSI for each land use type remained stable. The PLADJ and IJI of wetlands underwent significant changes from 2011 to 2012, as revealed in the previous Sankey diagram (Figure 5), indicating the emergence of wetlands in 2012 due to the conversion of a small amount of water into wetlands. After 2012, the aggregation degree and IJI of wetlands showed significant changes, with the aggregation degree gradually decreasing and the shape gradually becoming more uniform. Further analysis of barren land changes revealed a sharp decrease in aggregation degree from 2019 to 2020. Additionally, it can be seen that the LPI of cultivated land is much higher than that of other land uses and shows a decreasing trend each year, while the LPI of other land uses remains relatively stable. It can be seen that, since 2001, the urbanization process and ecological environment protection in the Haihe River Basin gradually tended toward a balance.

3.3. Response of Carbon Storage to LULC Changes

The land use map of the Haihe River Basin from 2000 to 2020, along with the corrected carbon density data, was utilized as input for the InVEST model to calculate the annual carbon storage (Figure 7). As depicted in Figure 7, carbon storage exhibited a notable decline from 2000 to 2001, followed by a relatively stable trend post-2001. Overlaying the dynamic attitude curve of land use types with Figure 8 reveals the alignment of the forest carbon storage curve with the dynamic attitude curve from 2000 to 2020. This synchronization is attributed to forests having a higher carbon density compared to other land use types, coupled with their extensive coverage in the Haihe River Basin.

3.4. Forecast of LULC in 2025

The LSTM model was utilized to predict land use data for the year 2020, and the results obtained from the CA-Markov model were listed for comparison. The Kappa coefficient was calculated by comparing the predictions with the actual land use data for 2020. The Kappa coefficient for LSTM was found to be 95.01%, while for CA-Markov, it was 93.37%. According to the Kappa coefficient, the LSTM model demonstrated an improvement of nearly 2.00% in simulation accuracy compared to CA-Markov, indicating a higher level of reliability. Figure 9 illustrates that the prediction errors made by CA-Markov are primarily concentrated on the water portion in the middle of the image. In contrast, the errors made by LSTM are mainly focused on the utilization of other land parts at the edge of the image.

Subsequently, the LSTM model was employed to predict land use in 2025, as shown in Figure 10. In 2025, the predominant land use types are cultivated land, grassland, and forest. Significant expansions are anticipated for grassland and forest areas, while cultivated land and water are expected to diminish (Table 4). These observations highlight the improving ecological environment under the influence of sustainable development, emphasizing the ongoing importance of water resource management in the basin's future.

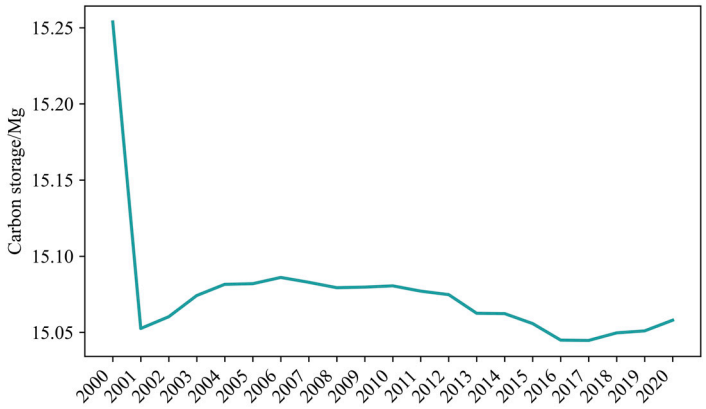

Figure 7. Carbon storage of Haihe River Basin.

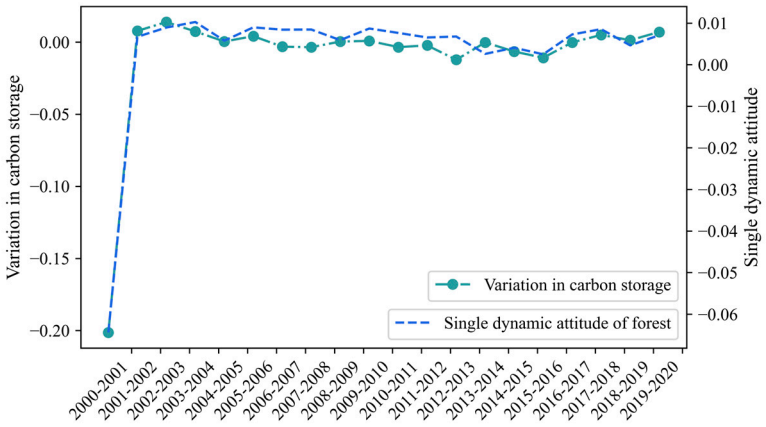

Figure 8. Variation in carbon storage of Haihe River Basin.

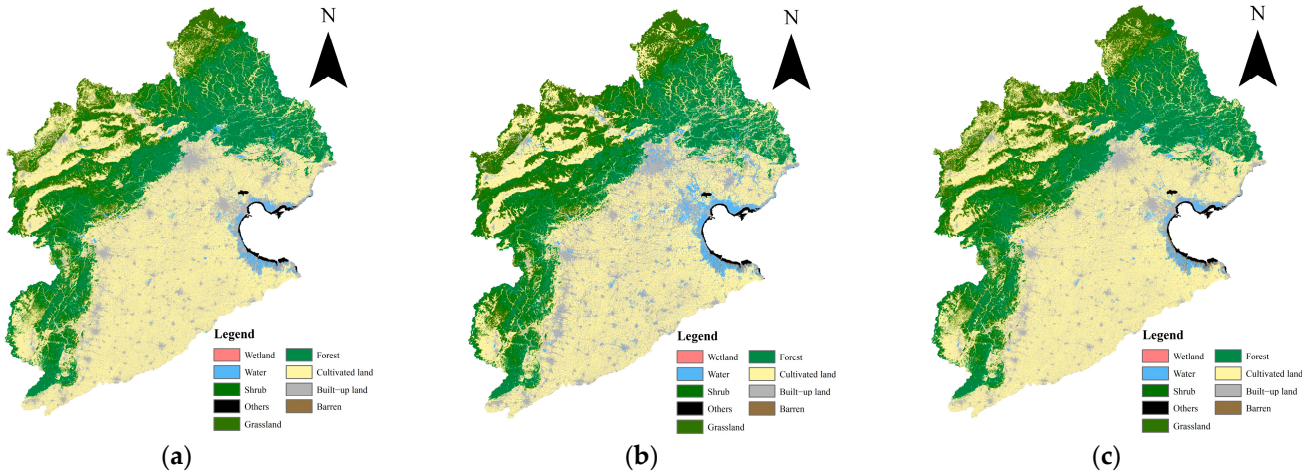

Figure 9. (**a**) Real LULC in 2020; (**b**) forecast by CA-Markov in 2020; (**c**) forecast by LSTM in 2020.

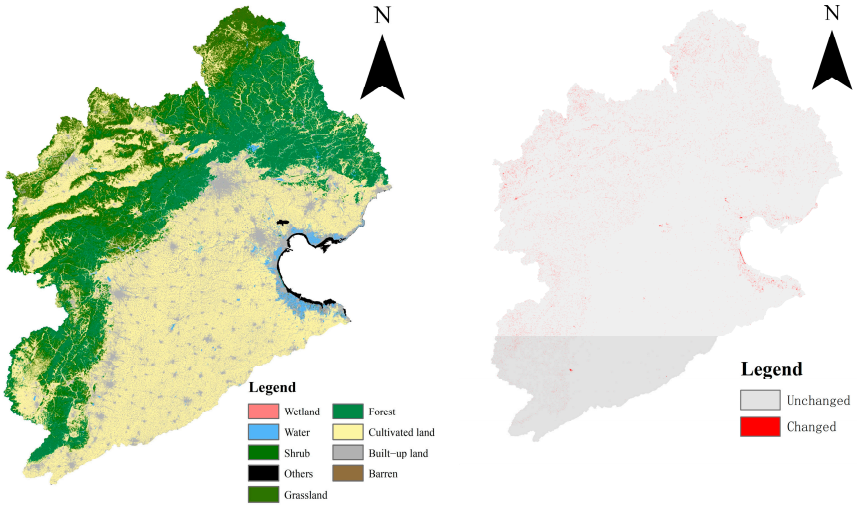

(**a**) (**b**)

Figure 10. (**a**) Distribution of LULC in Haihe River Basin in 2025; (**b**) change map of land use distribution in Haihe River Basin from 2020 to 2025.

Table 4. Future area of LULC in 2025 (ha).

LULC	Others	Forest	Water	Built-Up Land	Shrub	Grassland	Barren	Wetland	Cultivated Land
2020	172,554	6,923,916	449,089	4,547,813	121,522	5,438,430	27,463	16	14,836,740
2025	172,688	6,936,629	435,200	4,542,484	115,783	5,565,429	23,726	16	14,725,588
	+134	+12,713	−13,889	−5329	−5739	+126,999	−3737	0	−111,152

3.5. Forecast of Carbon Storage in 2025

Building upon the prediction of land use in Haihe River Basin for 2025 (as illustrated in Section 3.4), the carbon storage distribution was forecast using the InVEST model 3.14.0. Figure 11 shows that the distribution of carbon storage in Haihe River Basin in 2025 is still high in the northwest and low in the southeast, but this value will change greatly compared with that in 2020. In 2020, the carbon storage range is 0–31.38 Mg, and in 2025, the carbon storage range will expand to 0–348.61 Mg. This significant increase is attributed to the significant expansion of grassland and forest areas in 2025, which have more carbon intensity compared to other land use types and can also be seen as a healthy future ecosystem in the Haihe River basin.

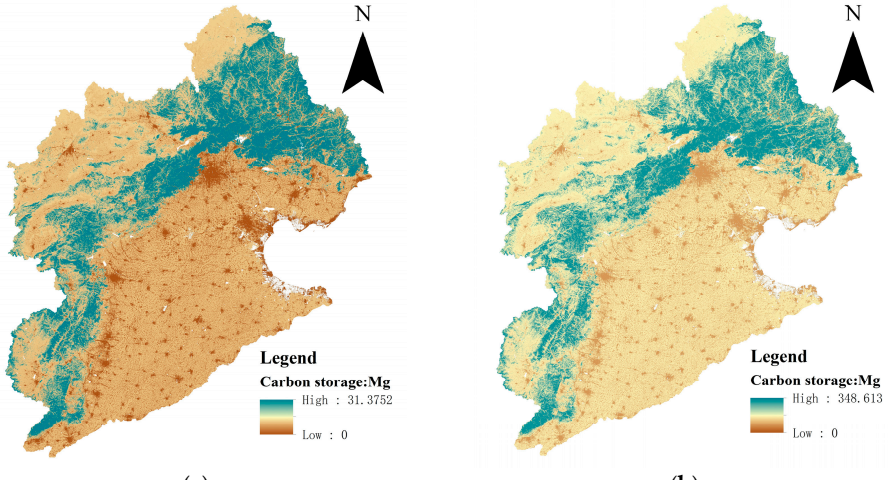

(**a**) (**b**)

Figure 11. (**a**) Carbon storage distribution map of Haihe River Basin in 2020; (**b**) carbon storage distribution map of Haihe River Basin in 2025.

4. Discussion

4.1. The Balance between the Urbanization Process and Sustainable Development in Haihe River Basin

In this study, the MK trend analysis, comprehensive dynamic attitude, and single dynamic attitude were employed to investigate the changes in land use reserves within the Haihe River Basin over the past 20 years. The most notable finding is the significant decrease in cultivated land area alongside a substantial increase in built-up land. The primary observed land use change involves the mutual conversion of forest, grassland, and cultivated land, along with the conversion of cultivated land to construction land, aligning with the findings of Fu Jiayi et al. [33]. According to the analysis results of comprehensive dynamic attitude, single dynamic attitude, and landscape indices, the Haihe River Basin can be roughly divided into two periods: 2000 to 2001 and 2001 to 2020. From 2000 to 2001, the growth rate of construction land notably declined, and the rate of forest reduction also slowed to some extent. Despite the national emphasis on sustainable development during this period, heavy industrialization and accelerating urbanization processes led to ecological damage. From 2002 to 2020, the urbanization process and ecological environmental protection in the Haihe River Basin gradually achieved a balance, leading to a stabilized land use transformation. Moreover, unsustainable rapid urbanization not only triggered land use alterations but also contributed to land fragmentation and dispersal, thereby threatening biodiversity and ecosystem health. Consequently, the meticulous planning and regulation of future urban expansion are imperative.

Additionally, LSTM was utilized to forecast the land use distribution of the Haihe River Basin in 2025. The projection suggests a significant increase in forest and grassland areas, accompanied by a decrease in water bodies. This forecast indicates a trend towards a healthier ecosystem within the Haihe River Basin. However, the ongoing monitoring of water resources in the basin remains an urgent task. Building upon this analysis, the integrated InVEST model determines the spatial distribution of future carbon stocks in the Haihe River Basin. The findings indicate a consistent pattern from 2020 to 2025, characterized by a high northwest and low southeast distribution. Furthermore, the majority of carbon stocks exhibit a stable pattern, consistent with the research conducted by Ji Xinhui et al. [34] and Wang Chao et al. [28].

4.2. Water Resource Management in the Haihe River Basin

The Haihe River Basin grapples with numerous ecological and environmental hurdles, including severe water scarcity, groundwater overexploitation, and wetland degradation. Thus, monitoring changes in water bodies and wetlands within the watershed is paramount. The research reveals that the expansion of the water area in the Haihe River Basin from 2000 to 2020 primarily stems from the reclamation of wasteland. Furthermore, some water bodies transformed wetlands in 2012, underscoring the efficacy of initiatives such as the South-to-North Water Diversion Project and the water-saving policies implemented by basin water management authorities in recent years. Notably, the period from 2018 to 2020 witnessed a substantial increase in the growth rate of water bodies, attributed to the proactive implementation of comprehensive "one reduction, one increase" management strategies by the Haihe River Commission and the Beijing–Tianjin–Hebei region since 2018.

4.3. Reflection on Study Limitations and Challenges

When calculating the carbon density of various land use types, the lack of precise measured data on carbon density introduces discrepancies in carbon storage predictions. While this study observes a similar trend in carbon storage change to that of Ji Xinhui et al. [34], there is a substantial disparity in carbon storage values. This variance is attributed to differences in the estimation of carbon density between cultivated land and forest grassland. Unlike Ji's assumption that the carbon density of cultivated land mirrors that of forest grassland, this study contends that forest grassland exhibits a higher carbon density, accounting for the inclusion of dead carbon density for each land use type. To enhance the accuracy of carbon storage research, future studies outlined in this paper will incorporate more comprehensive and precise

carbon density datasets. Moreover, additional climate factors will be considered for correction to bolster the reliability of the results.

Furthermore, in predicting land use, this paper solely considers the Digital Elevation Model (DEM), slope, and select traffic factors. This limited scope, coupled with inherent model errors, may constrain the accuracy of the prediction model in this study. Hence, further enhancements will necessitate the inclusion of additional drivers, alongside the development of higher-precision predictive models, to augment the predictive capacity of the models.

5. Conclusions

Through investigating the LULC changes and analyzing carbon storage in the Haihe River Basin over the past two decades using MK trend analysis, comprehensive dynamic attitude, and single dynamic attitude, we found that, from 2000 to 2020, cultivated land was the land use type with the most transferred area and built-up land was the land use type with the most significant area change in the Haihe River Basin. Water and wetland areas are increasing and the shape complexity is deepening. The overall trend of carbon storage in Haihe River Basin is declining, which reflects the acceleration of the urbanization process and the effective implementation of water environment regulation policies in the past 20 years. Compared with CA-Markov, the prediction accuracy of LSTM is improved by nearly 2.00%, reaching 95.01%. According to the LSTM model, the land use types of the Haihe River Basin in 2025 are still mainly cultivated land, forest, grassland, and built-up land. The mutual conversion between forest, grassland, and cultivated land will lead to a significant increase in forest and grassland areas, coupled with a decrease in cultivated land area from 2020 to 2025. Consequently, the carbon storage in the Haihe River Basin is projected to increase approximately tenfold by 2025 compared to 2020. In sum, LULC changes will change the structure of the ecosystem, and then affect the carbon storage. Understanding and monitoring the changes in LULC and carbon storage can allow for a timely assessment of the health status of the regional ecosystem, followed by the formulation of appropriate protection measures to promote local sustainable development and achieve the goal of "carbon neutrality and carbon peaking".

Author Contributions: Conceptualization, Y.L.; methodology, Y.L. and T.Y.; software, Y.L.; validation, Y.M.; formal analysis, Y.L.; investigation, Y.M. and T.Y.; data curation, Y.M. and T.Y.; writing—original draft preparation, Y.L.; writing—review and editing, L.C.; visualization, Y.L.; supervision, L.C.; project administration, L.C. All authors have read and agreed to the published version of the manuscript.

Funding: This research received no external funding.

Data Availability Statement: Data is contained within the article.

Conflicts of Interest: The authors declare no conflict of interest.

References

1. Wang, C.; Li, T.; Guo, X.; Xia, L.; Lu, C.; Wang, C. Plus-InVEST Study of the Chengdu-Chongqing Urban Agglomeration's Land-Use Change and Carbon Storage. *Land* **2022**, *11*, 1617. [CrossRef]
2. Ren, D.-F.; Cao, A.-H.; Wang, F.-Y. Response and Multi-Scenario Prediction of Carbon Storage and Habitat Quality to Land Use in Liaoning Province, China. *Sustainability* **2023**, *15*, 4500. [CrossRef]
3. Ge, Q.; Dai, J.; He, F.; Pan, Y.; Wang, M. Land use changes and their relations with carbon cycles over the past 300 a in China. *Sci. China Ser. D Earth Sci.* **2008**, *51*, 871–884. [CrossRef]
4. Ansari, A.; Golabi, M.H. Prediction of spatial land use changes based on LCM in a GIS environment for Desert Wetlands—A case study: Meighan Wetland, Iran. *Int. Soil Water Conserv. Res.* **2019**, *7*, 64–70. [CrossRef]
5. Wang, X.; Bao, Y. Study on the methods of landuse dynamic change research. *Prog. Geogr.* **1999**, *18*, 83–89.
6. Li, H.; Wu, J. Use and misuse of landscape indices. *Landsc. Ecol.* **2004**, *19*, 389–399. [CrossRef]
7. Wang, Y.; Cheng, W. Dynamic Change and Trend Prediction of Land Use in Jingtai Country Based on FLUS Model. *Territ. Nat. Resour. Study* **2023**, *05*, 11–15. [CrossRef]
8. Liu, Y. Study on the Evolution and Simulation of Land Use Landscape Pattern in the Lvzhijiang River Basin. Master's Thesis, Yunnan University of Finance and Economics, Kunming, China, 2024. [CrossRef]

9. Lian, H.; Qu, Z.; Liu, C.; He, Y. Spatio-temporal variation of landscape pattern and response of windbreak and sand fixation service in Hexi corridor of northern sand fixation belt. *Chin. J. Appl. Ecol.* **2023**, *34*, 2518–2526. [CrossRef]
10. Du, H.; Mao, F.; Zhou, G.; Li, X.; Xu, X.; Ge, H.; Cui, L.; Liu, Y.; Zhu, D.; Li, Y. Estimating and Analyzing the Spatiotemporal Pattern of Aboveground Carbon in Bamboo Forest by Combining Remote Sensing Data and Improved BIOME-BGC Model. *IEEE J. Sel. Top. Appl. Earth Obs. Remote Sens.* **2018**, *11*, 2282–2295. [CrossRef]
11. Zhang, L.; Zhou, G.; Ji, Y.; Bai, Y. Spatiotemporal dynamic simulation of grassland carbon storage in China. *Sci. China Earth Sci.* **2016**, *59*, 1946–1958. [CrossRef]
12. Chu, L.; Zhang, X.; Wang, T.; Li, Z.; Cai, C. Spatial-temporal evolution and prediction of urban landscape pattern and habitat quality based on CA-Markov and InVEST model. *Chin. J. Appl. Ecol.* **2018**, *29*, 4106–4118. [CrossRef]
13. Piyathilake, I.D.; Udayakumara, E.P.; Ranaweera, L.V.; Gunatilake, S.K. Modeling predictive assessment of carbon storage using InVEST model in Uva province, Sri Lanka. *Model. Earth Syst. Environ.* **2022**, *8*, 2213–2223. [CrossRef]
14. Li, M.; Liang, D.; Xia, J.; Song, J.; Cheng, D.; Wu, J.; Cao, Y.; Sun, H.; Li, Q. Evaluation of water conservation function of Danjiang River Basin in Qinling Mountains, China based on InVEST model. *J. Environ. Manag.* **2021**, *286*, 112212. [CrossRef] [PubMed]
15. Huang, W.; Liu, H.; Luan, Q.; Jiang, Q.; Liu, J.; Liu, H. Detection and prediction of land use change in Beijing based on Remote Sensing and GIS. *Int. Arch. Photogramm. Remote Sens. Spat. Inf. Sci.* **2008**, *37*, 75–82.
16. Liu, M.; Hu, Y.; Chang, Y.; He, X.; Zhang, W. Land Use and Land Cover Change Analysis and Prediction in the Upper Reaches of the Minjiang River, China. *Environ. Manag.* **2009**, *43*, 899–907. [CrossRef]
17. Araya, Y.H.; Cabral, P. Analysis and Modeling of Urban Land Cover Change in Setúbal and Sesimbra, Portugal. *Remote Sens.* **2010**, *2*, 1549–1563. [CrossRef]
18. Park, S.; Jeon, S.; Choi, C. Mapping urban growth probability in South Korea: Comparison of frequency ratio, analytic hierarchy process, and logistic regression models and use of the environmental conservation value assessment. *Landsc. Ecol. Eng.* **2012**, *8*, 17–31. [CrossRef]
19. Wang, S.W.; Munkhnasan, L.; Lee, W.-K. Land use and land cover change detection and prediction in Bhutan's high altitude city of Thimphu, using cellular automata and Markov chain. *Environ. Chall.* **2021**, *2*, 100017. [CrossRef]
20. Li, F.; Han, H.; Yang, S. Analysis of Land Use Change in Gansu Province from 2000 to 2020 and Multi-scenario Simulation of Gansu's Ecological Space Based on PLUS. *Sci. Technol. Eng.* **2023**, *23*, 6316–6326.
21. Aburas, M.M.; Ahamad, M.S.S.; Omar, N.Q. Spatio-temporal simulation and prediction of land-use change using conventional and machine learning models: A review. *Environ. Monit. Assess.* **2019**, *191*, 205. [CrossRef]
22. Wei, M.; Du, C.; Wang, X. Analysis and Forecast of Land Use and Carbon Sink Changes in Jilin Province, China. *Sustainability* **2023**, *15*, 14040. [CrossRef]
23. Wang, J.; Yin, X.; Liu, S.; Wang, D. Study on the change and prediction of spatiotemporal pattern of land use in Manasi region based on deep learning. *Arid Zone Res.* **2023**, *40*, 69–77. [CrossRef]
24. Xing, W.; Qian, Y.; Guan, X.; Yang, T.; Wu, H. A novel cellular automata model integrated with deep learning for dynamic spatio-temporal land use change simulation. *Comput. Geosci.* **2020**, *137*, 104430. [CrossRef]
25. Zhou, Y.; Huang, C.; Wu, T.; Zhang, M. A novel spatio-temporal cellular automata model coupling partitioning with CNN-LSTM to urban land change simulation. *Ecol. Model.* **2023**, *482*, 110394. [CrossRef]
26. Qian, H.; Zhai, J.; Ma, M.; Zhao, Y.; Ling, M.; Wang, Q. Temporal and Spatial Variation of Vegetation Coverage and Its Driving Forces During the Growing Season in Haihe River Basin. *Res. Soil Water Conserv.* **2023**, *30*, 309–317. [CrossRef]
27. Xu, L.; He, N.; Yu, G. A dataset of carbon density in Chinese terrestrial ecosystems (2010s). *China Sci. Data* **2019**, *4*, 21. [CrossRef]
28. Wang, C.; Zhan, J.; Chu, X.; Liu, W.; Zhang, F. Variation in ecosystem services with rapid urbanization: A study of carbon sequestration in the Beijing–Tianjin–Hebei region, China. *Phys. Chem. Earth Parts A/B/C* **2019**, *110*, 195–202. [CrossRef]
29. Li, J.; Xia, S.; Yu, X.; Li, S.; Xu, C.; Zhao, N.; Wang, S. Evaluation of Carbon Storage on Terrestrial Ecosystem in Hebei Province Based on InVEST Model. *J. Ecol. Rural Environ.* **2020**, *36*, 854–861. [CrossRef]
30. Zheng, H.; Zheng, H. Assessment and prediction of carbon storage based on land use/land cover dynamics in the coastal area of Shandong Province. *Ecol. Indic.* **2023**, *153*, 110474. [CrossRef]
31. Wang, Z.; Wang, B.; Zhang, Y.; Zhang, Q. Dynamic simulation of multi-scenario land use change and carbon storage assessment in Hohhot city based on PLUS-InVEST model. *J. Agric. Resour. Environ.* **2023**, 1–18. [CrossRef]
32. Zhang, C.; Xiang, Y.; Fang, T.; Chen, Y.; Wang, S. Spatio-Temporal Evolution and Prediction of Carbon Storage in Taiyuan Ecosystem under the Influence of LUCC. *Saf. Environ. Eng.* **2022**, *29*, 248–258. [CrossRef]
33. Fu, J.; Zang, C.; Wu, W. Spatial and Temporal Variability Characteristics and Driving Mechanism of Land use in Haihe River Basin From 1990 to 2015. *Chin. J. Agric. Resour. Reg. Plan.* **2020**, *41*, 131–139.
34. Ji, X.; Cao, Y.; Yao, J.; Zhai, H.; Fan, J. Land use and ecosystem carbon storage change and prediction in the Haihe River basin. *South-North Water Transf. Water Sci. Technol.* **2023**, *21*, 985–995. [CrossRef]